Physics of Plasmas

RESEARCH ARTICLE | FEBRUARY 11 2025

Modulation of electron precipitation regulated by electron injection: PIC simulations

Zhenyu Kong ; Xinliang Gao ; Quanming Lu ; Wentian Lei ; Xueyi Wang ; Jiuqi Ma ; Yangguang Ke ; Junyi Ren

Phys. Plasmas 32, 022108 (2025)
https://doi.org/10.1063/5.0241061

Modulation of electron precipitation regulated by electron injection: PIC simulations

Cite as: Phys. Plasmas **32**, 022108 (2025); doi: 10.1063/5.0241061
Submitted: 28 September 2024 · Accepted: 28 January 2025 ·
Published Online: 11 February 2025

Zhenyu Kong,[1,2,3] Xinliang Gao,[1,2,3,4,a)] Quanming Lu,[1,2,3,4,b)] Wentian Lei,[1,2,3] Xueyi Wang,[5] Jiuqi Ma,[1,2,3] Yangguang Ke,[1,2,3] and Junyi Ren[1]

AFFILIATIONS

[1]Deep Space Exploration Laboratory, School of Earth and Space Sciences, University of Science and Technology of China, Hefei 230026, China
[2]CAS Key Laboratory of Geoscience Environment, School of Earth and Space Sciences, University of Science and Technology of China, Hefei 230026, China
[3]CAS Center for Excellence in Comparative Planetology, Hefei 230026, China
[4]Collaborative Innovation Center of Astronautical Science and Technology, Harbin 150001, China
[5]Physics Department, Auburn University, Auburn, Alabama 36849, USA

[a)]**Author to whom correspondence should be addressed:** gaoxl@mail.ustc.edu.cn
[b)]**Electronic mail:** qmlu@ustc.edu.cn

ABSTRACT

It is widely accepted that repetitive chorus waves are responsible for the internal modulation of pulsating auroras. Recent studies have indicated that the repetitive nature of chorus waves stems from continuous electron injection. By employing a one-dimensional general curvilinear plasma simulation code, we introduce periodic electron injection into the simulation system. This generates repetitive rising-tone chorus waves, subsequently resulting in periodic electron precipitation, which potentially contributes to the formation of pulsating auroras. There is a distinct one-to-one correlation between each chorus element and the prompt electron precipitation. Moreover, we find that such electron precipitations are primarily driven by nonlinear interactions with chorus elements via nonlinear interactions, specifically phase bunching. Our work suggests that electron injection can modulate the electron precipitation by controlling the repetition period of chorus waves, thereby potentially influencing the period of internal modulation of pulsating auroras.

I. INTRODUCTION

Pulsating auroras are periodic flickering phenomena that occur in the Earth's upper atmosphere, with durations ranging from a few seconds to several tens of seconds.[1–3] Pulsating auroras have a horizontal spatial scale of approximately 100 km and typically appear at an altitude of ∼100 km.[2,4] Pulsating auroras tend to occur on the nightside and equatorward boundaries of the auroral oval, but their coverage expands during the geoactive period, sometimes even up to the dayside.[5,6] The brightness variations of pulsating auroras manifest as a series of rapid quasiperiodic on–off flickers.[7] For example, during the recovery phase of magnetic storms, modulation at a frequency of ∼3 Hz, called internal modulation, is often observed, which is superimposed on slower on–off flickering.[7–9]

Pulsating auroras are caused by intermittent precipitation of electrons with energies ranging from several keV to tens of keV.[1,10–12] Currently, several mechanisms have been proposed to explain the precipitation of those electrons, among which the most promising mechanism is pitch-angle scattering by chorus waves via cyclotron resonance.[12–18] The typical amplitude of chorus waves in the magnetosphere is approximately tens of pT, and previous studies have shown that those chorus waves are able to precipitate 0.1–30 keV electrons into the upper atmosphere.[19–22] Moreover, joint observations from satellites and ground stations have provided compelling evidence for the close correlation between chorus elements and the internal modulation of pulsating auroras; that is, discrete elements of rising-tone chorus waves observed near the equator correspond well to individual bursts of pulsating auroras in the atmosphere.[23–26]

Recently, both simulations and satellite observations[27,28] have shown that repetitive chorus waves can be excited by electron injection from a plasma sheet and that the repetition period is modulated by the

speed of electron injection. Therefore, it is reasonable to speculate that the internal modulation of pulsating auroras may essentially be regulated by electron injection. In this study, with the one-dimensional general curvilinear plasma simulation code (1D GCPIC), we simulate the entire process, including both wave excitation and electron precipitation, and successfully reproduce the periodic electron precipitation (i.e., pulsating aurora) by injecting energetic electrons into this model. Moreover, we analyzed the interaction pattern between chorus waves and electrons, which is responsible for prompt precipitation. Our study provides new insights into the internal modulation of pulsating auroras.

II. SIMULATION MODEL

Numerical experiments are performed by using a 1D GCPIC with a dipole magnetic field [Fig. 1(a)]. The plasma in this model consists of background cold electrons, anisotropic hot electrons and stationary protons. The simulation domain follows a magnetic field line, covering the magnetic latitude (λ) range of $-27.5°$–$27.5°$ [Fig. 1(a)]. To optimize the computational efficiency, we configured the topology of the background magnetic field to emulate conditions at L = 0.5. Unlike previous PIC models,[29,30] this model allows continuous hot electrons to be injected into the system with a constant drift velocity that can be expressed by τ_D^{-1}, and its details have been described in Lu *et al.*[28] A smaller τ_D represents a greater velocity of electron injection. The absorbing boundary condition is applied for the electromagnetic field. For a particle encountering the simulation boundary, it will be removed if its pitch angle is smaller than the local loss cone angle; otherwise, it will be reflected. Here, a loss cone angle of 6.65° is estimated at the simulation boundary if the upper atmosphere is assumed to be at 1 Earth radius (the radius of Earth in the simulation has also been reduced by a factor of 10), where the particle precipitates [Fig. 1(a)].

Initially, hot electrons satisfy a bi-Maxwellian distribution, and their number density and temperature anisotropy at the equator are set to $n_{h,eq}/n_{c0} = 0.006$ and $T_{\perp,eq}/T_{\|,eq} = 5.5$ (n_{c0} is the number density of cold electrons, and $T_{\|,eq} = 0.5 m_e V_{th\|}^2$ is the parallel temperature, where $V_{th\|} = 0.2c$ is the parallel thermal velocity of hot electrons and c is the speed of light). The distribution of hot electrons along the magnetic field line satisfies the pressure equilibrium.[29,31,32] The cold electrons are isotropic at a temperature of 10 eV and are distributed uniformly in the simulation domain. The ratio of the plasma frequency to the electron gyrofrequency at the equator is set to $\omega_{pe}/\Omega_{e0} = 5.0$ (where $\omega_{pe} = \sqrt{n_0 e^2/m_e \varepsilon_0}$, $\Omega_{e0} = eB_0/m_e$, B_0 is the background magnetic field at the equator, and m_e is the electron mass). These plasma parameters are typical values at approximately L = 6 in the Earth's magnetosphere. There are 4000 grid cells and approximately 4000 particles per cell in the model. The time step is $0.03\Omega_{e0}^{-1}$, and the grid spacing is $0.34 d_e$ (where $d_e = c/\omega_{pe}$). In this study, we conducted three runs with $\tau_D\Omega_{e0} = 21\,000$ (Run 1), 12 000 (Run 2), and 6000 (Run 3) to generate chorus waves with different repetition periods.

III. RESULTS

Figures 1(b)–1(d) show the dynamic spectrograms of the fluctuating magnetic fields at $\lambda = 15°$ for runs 1–3. The rising-tone chorus waves are excited near the equator and then propagate toward higher latitudes and saturate at approximately $\lambda = 15°$. Because the evolution process is quite similar to that of previous simulation results,[29,33] it is not described in detail. Since there is a continuous supply of free energy for exciting chorus waves, the rising-tone chorus elements appear sequentially, with periods of approximately 0.83, 0.45, and 0.24 s for runs 1–3. These repetitive chorus waves are widely observed in the Earth's magnetosphere[21,27,34,35] and have also been successfully

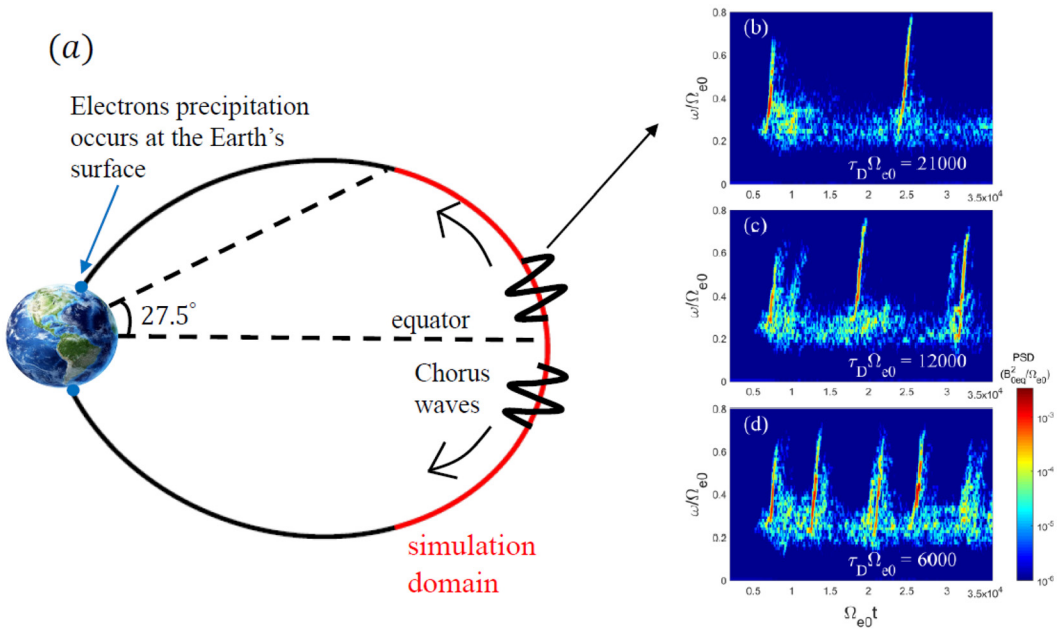

FIG. 1. (a) Diagram of electron precipitation into the Earth's atmosphere and chorus wave propagation. (b)–(d) Spectrograms of the power spectral density (PSD) of magnetic fields at latitude $\lambda = 15°$ in runs 1–3.

reproduced in self-consistent models.[28,36,37] As the injection speed of hot electrons (or the decrease in τ_D) increases, the period of repetitive chorus waves clearly tends to decrease, suggesting that the repetition period of chorus waves is controlled by the injection speed of hot electrons.[27]

Here, we focus on the electron precipitation caused by repetitive chorus waves. The removed electrons at the simulation boundaries represent electron precipitation into the polar upper atmosphere, and they are recorded for further analysis. Figures 2(a)–2(c) present the time evolution of the precipitating electron count for three runs. Overall, the electron precipitation in all runs occurs in the energy range of hundreds of eV to tens of keV, which can contribute to the formation of Earth's diffuse aurora.[1,4,12,23] Interestingly, the intensity of electron precipitation clearly shows a pulsating pattern with periods of ∼0.81, ∼0.42, and ∼0.22 s for runs 1–3. This period is quite similar to the period of pulsating auroras observed by ground-based stations.[7,9,25] To show the correlation between chorus waves and electron precipitation, we present the time profile of the wave amplitude (blue line) and the number of precipitating electrons (red lines) for runs 1–3 in Figs. 2(d)–2(f). The amplitudes of chorus waves are obtained by integrating the magnetic power spectral density from $0.1f_{ce}$ to $0.8f_{ce}$ at $\lambda = 15°$ (northern hemisphere). Since the corresponding electron precipitation occurs in the southern hemisphere, we accumulate the number of precipitating electrons for all energies at $\lambda = -27.5°$. In each run, the number of precipitating electrons exhibits a clear correlation with the wave amplitude, with the exception of a slight time delay [Figs. 2(d)–2(f)]. The time delay in runs 1–3 is estimated as $739\,\Omega_{e0}^{-1}$, $758.4\,\Omega_{e0}^{-1}$, and $652.8\,\Omega_{e0}^{-1}$, respectively, when the correlation coefficient between the time-shifted amplitude and the number of precipitating electrons reaches its peak value. The time delay is attributed to the flight time, which refers to the duration it takes for the electrons, after resonating with the chorus waves, to travel along the magnetic field lines until they precipitate at the simulation boundary. For instance, the flight time of electrons with energies ranging from 30 to 60 keV with the pitch angle of 45° falls within the range of 632–$814\,\Omega_{e0}^{-1}$, consistent with the estimated time delay. By considering the time delays, the correlation coefficients for runs 1–3 are 0.8927, 0.9144, and 0.8975, respectively. The high correlation (>0.89) supports that intensity-modulated chorus waves are responsible for driving the periodic electron precipitation.

To understand how chorus waves cause prompt electron precipitation, we have conducted a detailed analysis of wave–electron interactions. We select a representative of the precipitating electrons in run 1 and trace the electron trajectory during its lifetime. Figures 3(a)–3(c) show the time history of the magnetic latitude, equatorial pitch angle, and kinetic energy of the electron during the interval just before it precipitates. Before $\sim 7300\,\Omega_{e0}^{-1}$, this electron bounces back and forth in the dipole field, and its equatorial pitch angle and kinetic energy remain nearly unchanged. During the interval shaded in Figs. 3(b) and 3(c) around $t\Omega_{e0} = 7350$, the equatorial pitch angle of the electron

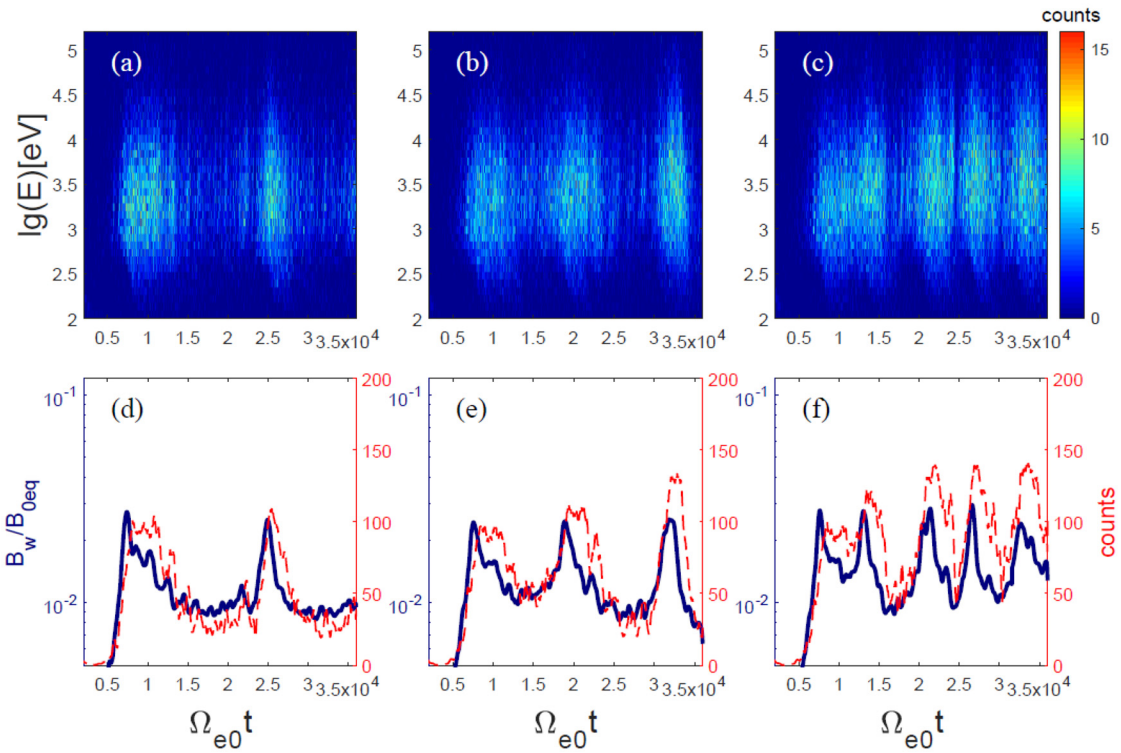

FIG. 2. (a)–(c) Temporal evolution of the counts of precipitating electrons with different energies observed at the boundary in the southern hemisphere for runs 1–3. (d)–(f) Temporal variation in the counts of all precipitating electrons observed at the boundary in the southern hemisphere for runs 1–3 (shown as red dashed lines) and fluctuating amplitudes (shown as blue solid lines). The fluctuating amplitudes are obtained by integrating the magnetic power spectral density at magnetic latitude $\lambda = 15°$ from frequencies $0.1f_{ce}$ to $0.8f_{ce}$.

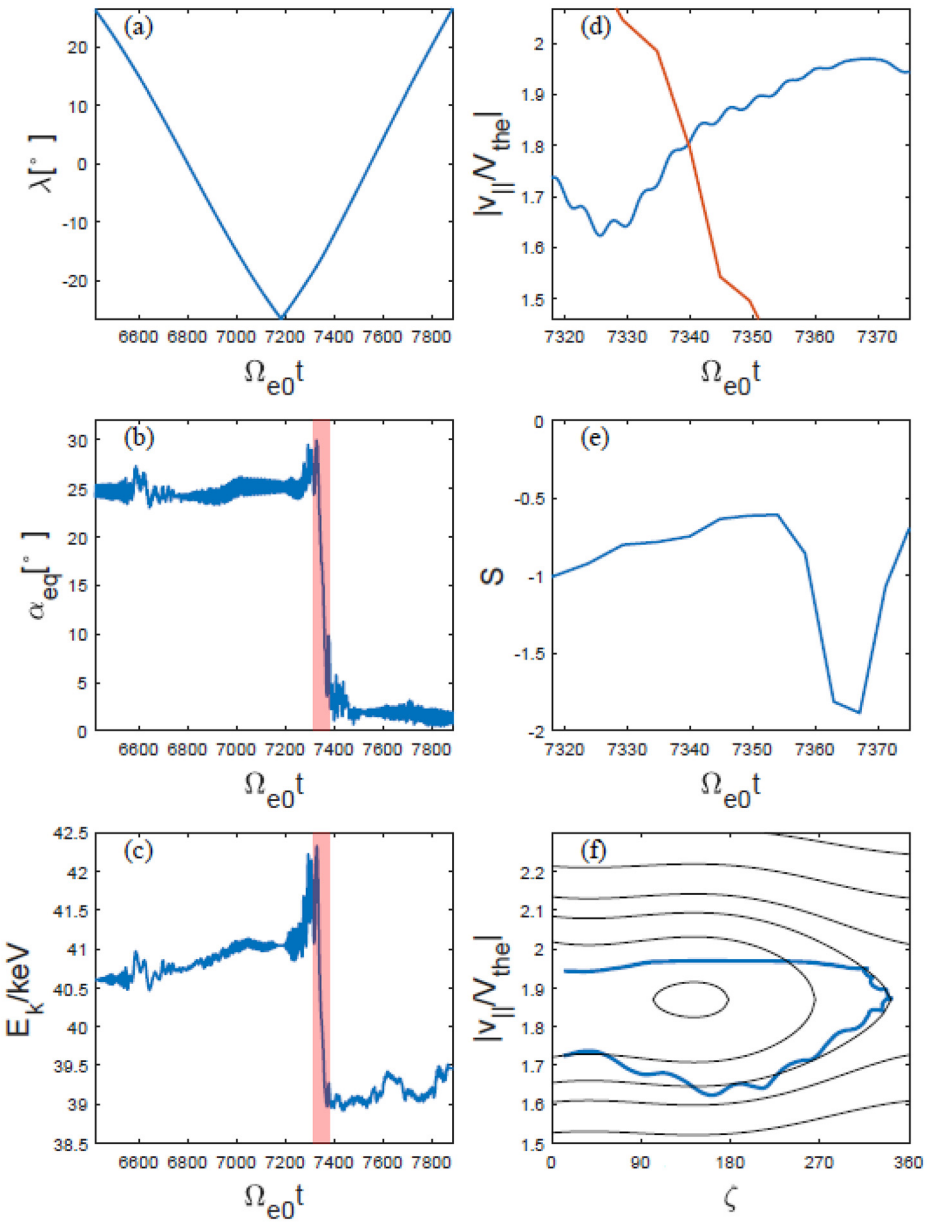

FIG. 3. Information on a selected precipitating electron. The temporal variations in (a) the electron's latitude, (b) the electron's equatorial pitch angle, and (c) the electron's energy. The red shaded area represents the period with the fastest changes in electron pitch angle and energy, as shown in Fig. 3(c). (d) Absolute value of the electron parallel velocity, (e) inhomogeneity factor S, and (f) trajectory of the electron in phase space during the selected period shown in Fig. 3(c).

rapidly decreases to ∼3° (smaller than the loss cone angle) and its kinetic energy decreases, causing this electron to precipitate into the north pole. Figure 3(d) presents the electron parallel velocity $v_{||}$ (blue line) and the cyclotron resonance velocity V_R (red line) during this interval. The resonance velocity V_R is calculated by

$$V_R = (\omega - \Omega_e)/k, \tag{1}$$

where ω is the wave frequency, Ω_e is the local electron gyrofrequency, and k is the wavenumber. The wave frequency ω is given by $\omega = 2\pi/T$ and the wave half periods $T/2$ inside each wave packet are calculated as the intervals between two consecutive zero crossings of the wave field. The wavenumber k is given by

$$k^2 = \frac{1}{c^2}\left(\omega^2 + \frac{\omega\omega_{pe}^2}{\Omega_e - \omega}\right), \tag{2}$$

based on the linear dispersion relation of whistler-mode waves. The cyclotron resonance condition is exactly satisfied at approximately $t\Omega_{e0} \approx 7340$.

To identify whether the wave–electron interaction is linear or nonlinear, we further present the inhomogeneity factor S and the trajectory of the electron in phase space in Figs. 3(e) and 3(f), respectively. The inhomogeneity factor S has been widely used to quantitively determine whether an electron undergoes a strong nonlinear interaction with a chorus wave.[30] The inhomogeneity factor S is given by

$$S = -\frac{1}{\omega_t^2 \chi^2}\left(\gamma\left(1-\frac{V_R}{V_g}\right)^2\frac{\partial\omega}{\partial t} + \left(\frac{k\gamma v_\perp^2}{2\Omega_e} - \left(1+\frac{\chi^2}{2}\frac{\Omega_e-\gamma\omega}{\Omega_e-\omega}\right)V_R\right)\frac{\partial\Omega_e}{\partial h}\right), \quad (3)$$

where V_g is the group velocity, $\omega_t = \sqrt{kv_\perp\Omega_w}$, $\Omega_w = eB_w/m_e$, B_w is the wave amplitude, $\chi = \sqrt{1-\omega^2/(c^2k^2)}$, $v_\perp$ is the perpendicular velocity of the electron, γ is the Lorentz factor, and h is the distance from the equator along the field line. When $|S|$ is less than 1, a strong nonlinear interaction occurs between the resonant electron and the chorus wave.[30] As shown in Fig. 3(e), $|S|$ remains below 1 at approximately $t\Omega_{e0} \approx 7340$ (when the cyclotron resonance condition is exactly satisfied), suggesting that the strong scattering of electrons is caused by nonlinear wave–electron interactions. On the basis of the nonlinear theoretical model, electrons undergoing nonlinear interactions may have two types of trajectories in phase space. The first type is the closed elliptical trajectory of phase-trapping electrons (type I), and the second type is the trajectory of phase bunching electrons moving outside the separatrix (type II).[30,38,39] In Fig. 3(f), the blue solid line represents the electron's trajectory in phase space, and the black solid lines depict the theoretical trajectories of resonant electrons that are described by the following equation:

$$\theta^2 + 2\omega_{tr}^2(\cos\zeta - S\zeta) = C, \quad (4)$$

where C is a constant, $\theta = k(v_{||} - V_R)$, $\omega_{tr} = \omega_t\chi\gamma^{-1/2}$, and ζ is the angle between the perpendicular component of the wave field and the perpendicular component of the electron velocity. Here, the inhomogeneity factor S ($S = -0.67$), wavenumbers k and ω_{tr} are the average values over the interval $t\Omega_{e0} = 7335$–7345 when cyclotron resonance occurs. The electron trajectory matches type II, i.e., just outside the closed separatrix (black bold line), suggesting phase bunching. Therefore, this electron undergoes nonlinear interactions with chorus waves, and the phase bunching effect leads to its loss/precipitation.

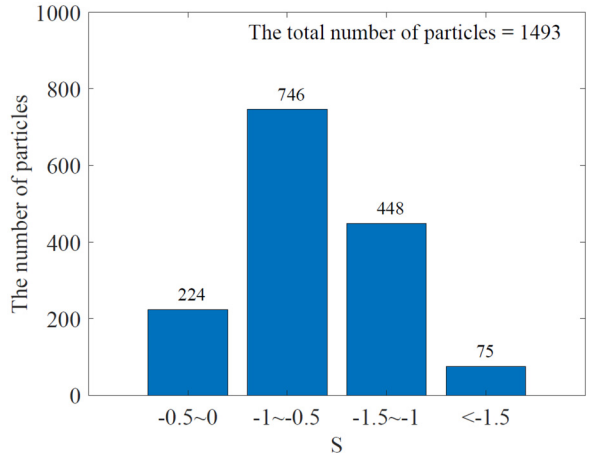

FIG. 4. Statistical value of the inhomogeneity factor S of precipitating electrons in the southern hemisphere within the time range $t\Omega_{e0} = 7800$–8000 in run 1.

We have also statistically analyzed the inhomogeneity factor S of the precipitating electrons in the southern hemisphere within the time range $t\Omega_{e0} = 7800$–8000 in run 1, as shown in Fig. 4. Notably, S is recorded for each electron when the cyclotron resonance condition is exactly satisfied. The majority of electrons experience strong nonlinear interactions with chorus waves before their precipitation, i.e., $|S| < 1$, and their pitch angles rapidly decrease due to the phase bunching effect. However, approximately one-third of the electrons with an inhomogeneity factor $|S|$ greater than 1 are precipitated, which may be partially attributed to the uncertainty of the selected plasma parameters. Then, we randomly select some precipitating electrons with $|S| > 1$ and find that both their equatorial pitch angles and energies rapidly decrease and that their trajectories in phase space support phase bunching (not shown). Therefore, we infer that almost all the precipitating electrons undergo a nonlinear process before their precipitation, as supported by the rapid decrease in electron pitch angle and energy and the motion trajectory in phase space.

IV. CONCLUSION

Observations have shown that repetitive chorus waves are capable of inducing periodic electron precipitation, which gives rise to the intermittent flickering characteristic of pulsating auroras. In addition, recent studies revealed that such repetitive chorus waves can be generated by electron injection. Therefore, it is reasonable to speculate that the internal modulation of the pulsating aurora may essentially be regulated by electron injection. In this study, we employed the 1D GCPIC to investigate the electron precipitation caused by self-consistently excited repetitive chorus waves. The simulation results clearly demonstrate that repetitive rising-tone chorus waves are generated by injected energetic electrons and then scatter electrons into the loss cone during propagation, causing repetitive electron precipitation, i.e., internal modulation of the pulsating aurora. There is a good one-to-one temporal correspondence between the chorus element and prompt electron precipitation, which is consistent with previous observations.[24–26] The prompt electron precipitation is due to a rapid decrease in the electron pitch angle, which is caused mainly by nonlinear wave–electron interactions, i.e., the phase bunching effect. On the basis of the simulation results, we propose that the injection velocity of energetic electrons controls the period of pulsating auroras by modulating the repetition period of chorus waves.

Previous simulations and observations have indicated that the drift velocity of hot electrons directly influences the repetition period of chorus waves.[27,28] In particular, Gao *et al.*[27] revealed that the day–night asymmetry of the Earth's magnetic field leads to different repetition periods of chorus waves on the day and night sides. Drawing from our simulation findings, we suggest that day–night asymmetry may also exist in the periodicity of pulsating auroras.

ACKNOWLEDGMENTS

This research was funded by NSFC Grant Nos. 42322406 and 42230201, Fundamental Research Funds for the Central Universities (KY2080000063 and KY2080000138), and the "USTC Tang Scholar" program. We also acknowledge the use of data resources from the National Space Science Data Center, National Science & Technology Infrastructure of China (http://www.nssdc.ac.cn).

AUTHOR DECLARATIONS

Conflict of Interest

The authors have no conflicts to disclose.

Author Contributions

Zhenyu Kong: Conceptualization (equal); Data curation (equal); Formal analysis (equal); Investigation (equal); Software (equal); Visualization (equal); Writing – original draft (equal). **Xinliang Gao:** Conceptualization (equal); Funding acquisition (equal); Methodology (equal); Project administration (equal); Resources (equal); Writing – review & editing (equal). **Quanming Lu:** Conceptualization (equal); Funding acquisition (equal); Resources (equal); Supervision (equal). **Wentian Lei:** Investigation (equal); Software (equal). **Xueyi Wang:** Software (equal); Validation (equal). **Jiuqi Ma:** Investigation (equal); Visualization (equal). **Yangguang Ke:** Software (equal); Visualization (equal). **Junyi Ren:** Data curation (equal); Software (equal).

DATA AVAILABILITY

The data that support the findings of this study are openly available in Science Data Bank at https://www.scidb.cn/detail?dataSetId=a349faf9699a457aaa37d523a7b30992 (Ref. 40).

REFERENCES

[1]A. D. Johnstone, "Pulsating aurora," Nature **274**, 119–126 (1978).
[2]M. Samara, R. G. Michell, and G. V. Khazanov, "First optical observations of interhemispheric electron reflections within pulsating aurora," Geophys. Res. Lett. **44**, 2618–2623, https://doi.org/10.1002/2017GL072794 (2017).
[3]G. T. Davidson, "Pitch-angle diffusion and the origin of temporal and spatial structures in morningside aurorae," Space Sci. Rev. **53**, 45–82 (1990).
[4]M. R. Lessard, in *Auroral Phenomenology and Magnetospheric Processes: Earth and Other Planets*, Geophysical Monograph Series (Annales Geophysicae, 2012), pp. 55–68.
[5]S. L. Jones, M. R. Lessard, K. Rychert, E. Spanswick, and E. Donovan, "Large-scale aspects and temporal evolution of pulsating aurora," J. Geophys. Res. **116**, A03214, https://doi.org/10.1029/2010JA015840(2011).
[6]A. D. Johnstone, "The mechanism of pulsating aurora," Ann. Geophys. **1**, 397–410 (1983).
[7]T. Yamamoto, "On the temporal fluctuations of pulsating auroral luminosity," J. Geophys. Res. **93**, 897–911, https://doi.org/10.1029/JA093iA02p00897 (1988).
[8]O. Royrvik and T. N. Davis, "Pulsating aurora: Local and global morphology," J. Geophys. Res. **82**, 4720–4740, https://doi.org/10.1029/JA082i029p04720 (1977).
[9]Y. Miyoshi, S. Saito, K. Seki, T. Nishiyama, R. Kataoka, K. Asamura, Y. Katoh, Y. Ebihara, T. Sakanoi, M. Hirahara *et al.*, "Relation between fine structure of energy spectra for pulsating aurora electrons and frequency spectra of whistler mode chorus waves," J. Geophys. Res., [Space Phys.] **120**, 7728–7736, https://doi.org/10.1002/2015JA021562 (2015).
[10]I. Sandahl, L. Eliasson, and R. Lundin, "Rocket observations of precipitating electrons over a pulsating aurora," Geophys. Res. Lett. **7**, 309–312, https://doi.org/10.1029/GL007i005p00309 (1980).
[11]D. J. Mcewen, E. Yee, B. A. Whalen, and A. W. Yau, "Electron energy measurements in pulsating auroras," Can. J. Phys. **59**, 1106–1115 (1981).
[12]Y. Miyoshi, Y. Katoh, T. Nishiyama, T. Sakanoi, K. Asamura, and M. Hirahara, "Time of flight analysis of pulsating aurora electrons, considering wave-particle interactions with propagating whistler mode waves," J. Geophys. Res. **115**, A10312, https://doi.org/10.1029/2009JA015127 (2010).
[13]F. V. Coroniti and C. F. Kennel, "Electron precipitation pulsations," J. Geophys. Res. **75**, 1279, https://doi.org/10.1029/JA075i007p01279 (1970).
[14]B. Ni, R. M. Thorne, Y. Y. Shprits, and J. Bortnik, "Resonant scattering of plasma sheet electrons by whistler-mode chorus: Contribution to diffuse auroral precipitation," Geophys. Res. Lett. **35**, L11106, https://doi.org/10.1029/2008GL034032 (2008).
[15]M. Hikishima, Y. Omura, and D. Summers, "Microburst precipitation of energetic electrons associated with chorus wave generation," Geophys. Res. Lett. **37**, L07103, https://doi.org/10.1029/2010GL042678 (2010).
[16]J. He, Y. Jin, F. Xiao, Z. He, C. Yang, Y. Xie, Q. He, C. Wang, X. Shang, S. Liu *et al.*, "The influence of various frequency chorus waves on electron dynamics in radiation belts," Sci. China Technol. Sci. **64**, 890–897 (2021).
[17]X. Gao, J. Ma, T. Shao, R. Chen, Y. Ke, and Q. Lu, "Why chorus waves are the dominant driver for diffuse auroral precipitation," Sci. Bull. **69**, 597–600 (2024).
[18]X. Fuliang, H. Huiyong, Z. Qinghua, W. Guanhong, and S. Xianghua, "Storm-time evolution of energetic electron pitch angle distributions by wave-particle interaction," Plasma Sci. Technol. **10**, 27 (2008).
[19]B. T. Tsurutani and E. J. Smith, "Two types of magnetospheric ELF chorus and their substorm dependences," J. Geophys. Res. **82**, 5112–5128, https://doi.org/10.1029/JA082i032p05112 (1977).
[20]W. Li, R. M. Thorne, J. Bortnik, X. Tao, and V. Angelopoulos, "Characteristics of hiss-like and discrete whistler-mode emissions," Geophys. Res. Lett. **39**, L18106, https://doi.org/10.1029/2012GL053206 (2012).
[21]X. Gao, W. Li, R. M. Thorne, J. Bortnik, V. Angelopoulos, Q. Lu, X. Tao, and S. Wang, "New evidence for generation mechanisms of discrete and hiss-like whistler mode waves," Geophys. Res. Lett. **41**, 4805–4811, https://doi.org/10.1002/2014GL060707 (2014).
[22]R. M. Thorne, "Radiation belt dynamics: The importance of wave-particle interactions," Geophys. Res. Lett. **37**, L22107, https://doi.org/10.1029/2010GL044990 (2010).
[23]S. Kasahara, Y. Miyoshi, S. Yokota, T. Mitani, Y. Kasahara, S. Matsuda, A. Kumamoto, A. Matsuoka, Y. Kazama, H. U. Frey *et al.*, "Pulsating aurora from electron scattering by chorus waves," Nature **554**, 337–340 (2018).
[24]M. Ozaki, K. Shiokawa, Y. Miyoshi, K. Hosokawa, S. Oyama, S. Yagitani, Y. Kasahara, Y. Kasaba, S. Matsuda, R. Kataoka *et al.*, "Microscopic observations of pulsating aurora associated with chorus element structures: Coordinated arase satellite-PWING observations," Geophys. Res. Lett. **45**(12), 125–134, https://doi.org/10.1029/2018GL079812 (2018).
[25]R. Chen, Y. Miyoshi, X. Gao, Q. Lu, B. T. Tsurutani, K. Hosokawa, T. Hori, Y. Ogawa, S.-I. Oyama, Y. Kasahara *et al.*, "Observational evidence for three time-scale modulations in the pulsating aurora," Geophys. Res. Lett. **51**, e2024GL108253, https://doi.org/10.1029/2024GL108253 (2024).
[26]K. Hosokawa, Y. Miyoshi, M. Ozaki, S. I. Oyama, Y. Ogawa, S. Kurita, Y. Kasahara, Y. Kasaba, S. Yagitani, S. Matsuda *et al.*, "Multiple time-scale beats in aurora: precise orchestration via magnetospheric chorus waves," Sci. Rep. **10**, 3380 (2020).
[27]X. Gao, R. Chen, Q. Lu, L. Chen, H. Chen, and X. Wang, "Observational evidence for the origin of repetitive chorus emissions," Geophys. Res. Lett. **49**, e2022GL099000, https://doi.org/10.1029/2022GL099000 (2022).
[28]Q. Lu, L. Chen, X. Wang, X. Gao, Y. Lin, and S. Wang, "Repetitive emissions of rising-tone chorus waves in the inner magnetosphere," Geophys. Res. Lett. **48**, e2021GL094979, https://doi.org/10.1029/2021GL094979 (2021).
[29]Q. Lu, Y. Ke, X. Wang, K. Liu, X. Gao, L. Chen, and S. Wang, "Two-dimensional gcPIC simulation of rising-tone chorus waves in a dipole magnetic field," J. Geophys. Res., [Space Phys.] **124**, 4157–4167, https://doi.org/10.1029/2019JA026586 (2019).
[30]Y. Omura, Y. Katoh, and D. Summers, "Theory and simulation of the generation of whistler-mode chorus," J. Geophys. Res. **113**, A04223, https://doi.org/10.1029/2007JA012622 (2008).
[31]D. Summers, Y. Omura, Y. Miyashita, and D.-H. Lee, "Nonlinear spatiotemporal evolution of whistler mode chorus waves in Earth's inner magnetosphere," J. Geophys. Res. **117**, A09206, https://doi.org/10.1029/2012JA017842 (2012).
[32]X. Wang, H. Chen, Y. Omura, Y.-K. Hsieh, L. Chen, Y. Lin, X.-J. Zhang, and Z. Xia, "Resonant electron signatures in the formation of chorus wave subpackets," Geophys. Res. Lett. **51**, e2023GL108000, https://doi.org/10.1029/2023GL108000 (2024).
[33]Z. Kong, X. Gao, Y. Ke, Q. Lu, and X. Wang, "Simulation of chorus wave excitation in the compressed/stretched dipole magnetic field," J. Geophys. Res., [Space Phys.] **128**, e2022JA030779, https://doi.org/10.1029/2022JA030779 (2023).

[34]W. Li, R. M. Thorne, J. Bortnik, Y. Y. Shprits, Y. Nishimura, V. Angelopoulos, C. Chaston, O. Le Contel, and J. W. Bonnell, "Typical properties of rising and falling tone chorus waves," Geophys. Res. Lett. **38**, L14103, https://doi.org/10.1029/2011GL047925 (2011).
[35]J.-H. Shue, Y.-K. Hsieh, S. W. Y. Tam, K. Wang, H. S. Fu, J. Bortnik, X. Tao, W.-C. Hsieh, and G. Pi, "Local time distributions of repetition periods for rising tone lower band chorus waves in the magnetosphere," Geophys. Res. Lett. **42**, 8294–8301, https://doi.org/10.1002/2015GL066107 (2015).
[36]Z. Kong, X. Gao, Q. Lu, and X. Wang, "Generation mechanisms of Hiss-like chorus in the Earth's magnetosphere," J. Geophys. Res., [Space Phys.] **128**, e2023JA031711, https://doi.org/10.1029/2023JA031711 (2023).
[37]H. Chen, X. Wang, L. Chen, Y. Omura, B. T. Tsurutani, Y. Lin, and Z. Xia, "Evolution of chorus subpackets in the Earth's magnetosphere," Geophys. Res. Lett. **50**, e2023GL105938, https://doi.org/10.1029/2023GL105938 (2023).
[38]H. Chen, X. Wang, L. Chen, X.-J. Zhang, Y. Omura, R. Chen, Y.-K. Hsieh, Y. Lin, and Z. Xia, "Nonlinear electron trapping through cyclotron resonance in the formation of chorus subpackets," Geophys. Res. Lett. **51**, e2024GL109481, https://doi.org/10.1029/2024GL109481 (2024).
[39]H. Chen, X. Wang, H. Zhao, Y. Lin, L. Chen, Y. Omura, R. Chen, and Y.-K. Hsieh, "Electron dynamics associated with advection and diffusion in self-consistent wave-particle interactions with oblique chorus waves," Geophys. Res. Lett. **51**, e2024GL110362, https://doi.org/10.1029/2024GL110362 (2024).
[40]Z. Kong (2024). "The internal modulation of pulsating aurora regulated by the electron injection [DS/OL]. V2," Science Data Bank. https://doi.org/10.57760/sciencedb.10486